ASTHMA

Transgelin-2 as a therapeutic target for asthmatic pulmonary resistance

Copyright © 2018 The Authors, some rights reserved; exclusive licensee American Association for the Advancement of Science. No claim to original U.S. Government Works

Lei-Miao Yin,[1] Yu-Dong Xu,[1] Ling-Ling Peng,[1] Ting-Ting Duan,[1] Jia-Yuan Liu,[1] Zhijian Xu,[2] Wen-Qian Wang,[1] Nan Guan,[1] Xiao-Jie Han,[1] Hai-Yan Li,[1] Yu Pang,[1] Yu Wang,[1] Zhaoqiang Chen,[2] Weiliang Zhu,[2] Linhong Deng,[3] Ying-Li Wu,[4] Guang-Bo Ge,[5] Shuang Huang,[1,6] Luis Ulloa,[7,8]* Yong-Qing Yang[1]*

There is a clinical need for new bronchodilator drugs in asthma, because more than half of asthmatic patients do not receive adequate control with current available treatments. We report that inhibition of metallothionein-2 protein expression in lung tissues causes the increase of pulmonary resistance. Conversely, metallothionein-2 protein is more effective than β_2-agonists in reducing pulmonary resistance in rodent asthma models, alleviating tension in tracheal spirals, and relaxing airway smooth muscle cells (ASMCs). Metallothionein-2 relaxes ASMCs via transgelin-2 (TG2) and induces dephosphorylation of myosin phosphatase target subunit 1 (MYPT1). We identify TSG12 as a nontoxic, specific TG2-agonist that relaxes ASMCs and reduces asthmatic pulmonary resistance. In vivo, TSG12 reduces pulmonary resistance in both ovalbumin- and house dust mite–induced asthma in mice. TSG12 induces RhoA phosphorylation, thereby inactivating the RhoA-ROCK-MYPT1-MLC pathway and causing ASMCs relaxation. TSG12 is more effective than β_2-agonists in relaxing human ASMCs and pulmonary resistance with potential clinical advantages. These results suggest that TSG12 could be a promising therapeutic approach for treating asthma.

INTRODUCTION

Asthma is a common, chronic respiratory disease affecting more than 300 million people worldwide (*1*). Even in America and despite pharmaceutical advances, asthma affects more than 40 million people, representing about 10% of the population, and causing more than 2 million emergency visits and 500,000 hospitalizations every year according to the Centers for Disease Control and Prevention (*2*). The estimated total cost of asthma in America was more than $56 billion in 2007 (*3*), and the lifetime of the asthma population increased by more than 28% during 2001 to 2015. Asthma is a modern clinical challenge and a major economic burden in need for effective treatments.

Asthma is characterized by recurrent episodes of wheezing, chest tightness, pulmonary obstruction, and respiratory insufficiency (*4*). Although asthma is believed to be an allergic, eosinophilic, and T helper 2 cell (T_H2)–mediated disease, about 50% of patients show no evidence of a T_H2 phenotype, and this phenotype does not correlate with the clinical symptoms (*5*). Moreover, T_H2-focused clinical trials reduced inflammation but produced limited therapeutic benefits, suggesting that asthma is a complex process converging in the narrowing of the airways and subsequent pulmonary resistance (*6*, *7*). Thus, some current studies focus on relaxing airway smooth muscle cells (ASMCs) in asthma (*8*–*10*). Given the role of the smooth muscles in narrowing the airways, ASMCs relaxation can be a promising therapeutic strategy for pulmonary resistance in asthma (*9*, *11*).

Despite its clinical implications, the etiology and mechanism of ASMCs contraction in asthma are not well known (*9*). The conventional U.S. Food and Drug Administration (FDA)–approved treatments for asthma include inhaled β_2-agonists that exert therapeutic effects through β_2-adrenoceptors; however, more than half of asthmatic patients do not receive adequate control with current available agents (*12*–*14*). β_2-adrenoceptors are susceptible to desensitization, and patients can become less sensitive and unresponsive over time, leaving them with persistent and uncontrolled symptoms (*15*, *16*). β_2-agonists also have deleterious side effects, increasing the risk of morbidity (*17*, *18*). β_2-agonists are often combined with corticosteroids, but corticosteroids also increase the risk of respiratory infections, such as yeast infections in thrush, and cause detrimental side effects, including immunosuppression (*19*, *20*). Therefore, there is a clinical unmet need to design new bronchodilator drugs to relax ASMCs and reduce pulmonary resistance in asthma.

Metallothionein-2 (MT-2) is a member of the metallothionein family of proteins that is highly conserved through evolution and is expressed in mammalian airway epithelial cells and the smooth muscle cells (*21*, *22*). Although metallothioneins protect against pulmonary oxidative stress during endotoxemia (*23*), MT-2 has not been studied in asthma. Here, we report that MT-2 ameliorates asthmatic pulmonary resistance by relaxing ASMCs via transgelin-2 (TG2). Structural analyses allowed us to identify TSG12 as a nontoxic, specific TG2 agonist that is more effective than β_2-agonists in relaxing human ASMCs and reducing pulmonary resistance in asthma.

RESULTS

MT-2 reduces asthmatic pulmonary resistance

To study the pathogenesis of asthma, we analyzed MT-2 protein in lung tissues of ovalbumin (OVA)–induced asthmatic rats. MT-2 protein levels were consistently more than 50% lower in asthmatic lung tissues than

[1]Yueyang Hospital, Shanghai University of Traditional Chinese Medicine, Shanghai 200030, China. [2]Chinese Academy of Sciences Key Laboratory of Receptor Research, Drug Discovery and Design Center, Shanghai Institute of Materia Medica, Chinese Academy of Sciences, Shanghai 201203, China. [3]Institute of Biomedical Engineering and Health Sciences, Changzhou University, Jiangsu 213164, China. [4]Department of Pathophysiology, Shanghai Jiao Tong University School of Medicine, Shanghai 200025, China. [5]Institute of Interdisciplinary Medicine, Shanghai University of Traditional Chinese Medicine, Shanghai 200030, China. [6]Department of Biochemistry and Molecular Biology, Medical College of Georgia, Georgia Regents University, Augusta, GA 30912, USA. [7]International Laboratory of Neuro-Immunomodulation, Shanghai University of Traditional Chinese Medicine, Shanghai 200030, China. [8]Department of Surgery, Center of Immunology and Inflammation, Rutgers New Jersey Medical School, Newark, NJ 07101, USA.
*Corresponding author. Email: yyq@shutcm.edu.cn (Y.-Q.Y.); luis.ulloa@rutgers.edu (L.U.)

Downloaded from http://stm.sciencemag.org/ by guest on July 7, 2021

in control samples (Fig. 1A). This result suggested that inhibition of MT-2 expression may contribute to asthma. Metallothionein proteins are highly conserved, cysteine-rich proteins expressed in pulmonary endothelial cells (*24*). Given that previous studies reported that metallothioneins protect against pulmonary oxidative stress during endotoxemia (*23*), we reasoned that inhibition of metallothionein protein expression can contribute to pulmonary resistance in asthma. We tested this hypothesis by analyzing whether metallothionein knockout (MT-KO) mice are more susceptible to asthma. MT-KO mice have about twofold higher pulmonary resistance than wild-type OVA-induced asthmatic mice (Fig. 1B).

Conversely, we reasoned that application of recombinant MT-2 may reduce pulmonary resistance in asthma. We purified MT-2 recombinant protein by affinity chromatography in nickel–nitrilotriacetic acid (Ni-NTA) columns to treat OVA-induced asthmatic rats (Fig. 1C). Injection of recombinant MT-2 through an external jugular vein reduced pulmonary resistance in asthmatic rats (Fig. 1D). We also compared the efficacy of MT-2 with conventional FDA-approved treatments, including β_2-agonists and hydrocortisone. By comparison, a dose of MT-2 (0.1 μg/kg) elicited smooth muscle relaxation similar to that of terbutaline (55 μg/kg) or hydrocortisone (15 mg/kg). MT-2 was more effective than terbutaline or corticosteroid in reducing pulmonary resistance in asthmatic rats (Fig. 1D). Time-course analyses also showed that MT-2 induced a clinically relevant rapid response, decreasing pulmonary resistance within the first 3 to 8 min after administration (fig. S1).

We also analyzed whether MT-2 reduces isometric tension in rat isolated tracheal spirals. Tracheal spirals were challenged with acetylcholine (10^{-5} M) to induce 70 to 75% of the maximal contractile response (*25*) and then treated with MT-2 or terbutaline. MT-2 significantly reduced the isometric tension of rat tracheal spirals by more than 60% ($P < 0.05$; Fig. 1E). Again, MT-2 was more effective than the β_2-agonist terbutaline. A dose of 30 nM MT-2 elicits a smooth muscle relaxation 1.5-fold higher than that of 1500 nM terbutaline. At the cellular level, MT-2 inhibited ASMCs contraction induced by collagen. MT-2 significantly relaxed primary rat ASMCs in a dose-dependent manner in the collagen gel contraction assay ($P < 0.05$; Fig. 1F). This effect was not limited to the ASMCs contraction induced by collagen, because MT-2 also inhibited acetylcholine-induced contraction of primary rat ASMCs (Fig. 1G). Primary rat ASMCs were then treated with MT-2 and challenged with acetylcholine. MT-2 was more effective than terbutaline in relaxing primary rat ASMCs (Fig. 1G). Thus, we reasoned that the MT-2 receptor responsible for relaxing ASMCs can be a therapeutic target for pulmonary resistance in asthma.

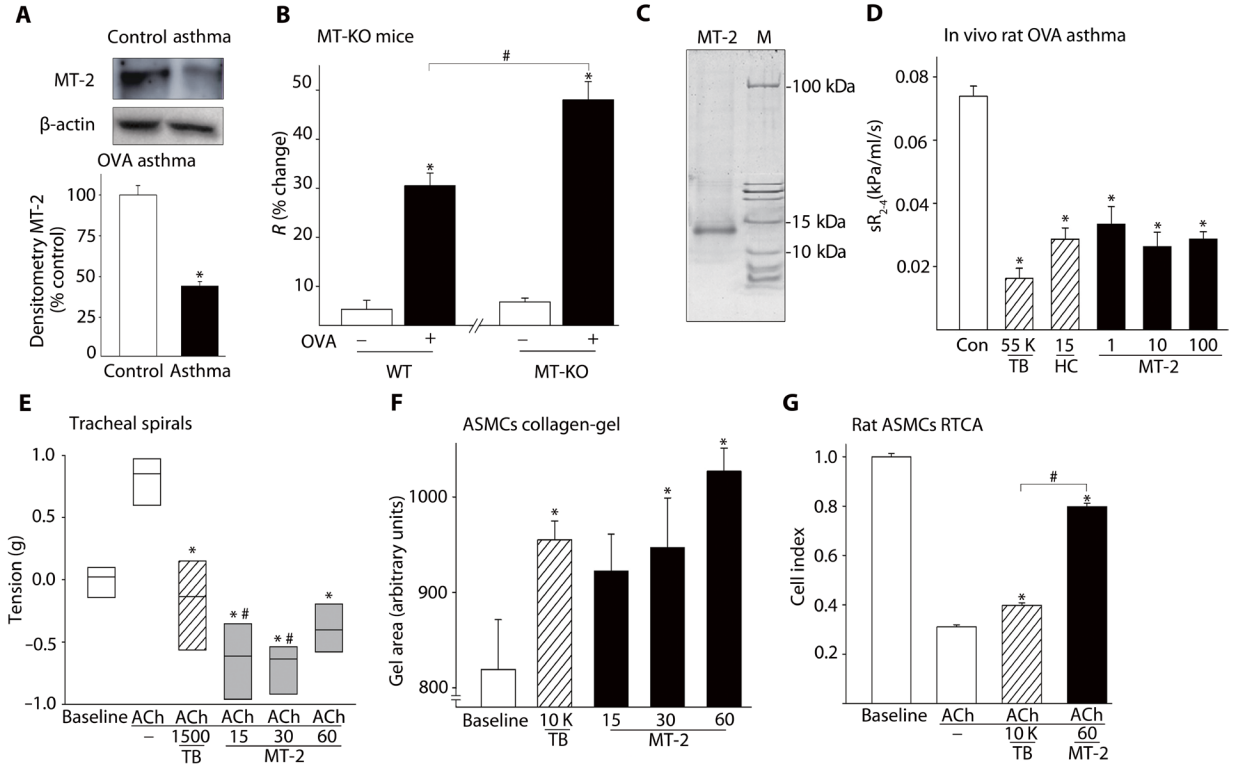

Fig. 1. MT-2 ameliorates asthmatic pulmonary resistance. (**A**) Western blot analyses of metallothionein-2 (MT-2) protein in control and asthmatic lung tissues from ovalbumin (OVA)–sensitized and OVA-challenged rats. Lower panel: Mean density of MT-2 normalized to β-actin (*$P < 0.05$ versus control, *t* test; $n = 5$ per group). (**B**) Pulmonary resistance (*R*) in wild-type (WT) and metallothionein knockout (MT-KO) OVA-sensitized mice challenged with vehicle (control) or OVA. (*$P < 0.05$ versus control and $^{\#}P < 0.05$ versus WT mice challenged with OVA, $n = 8$ per group). (**C**) Gel of purified rat MT-2 recombinant protein and molecular weight markers (M). (**D**) Pulmonary resistance peak value sum of 2 to 4 min (sR_{2-4}) for OVA-challenged rats without treatment (Con) or treated with terbutaline (TB; 0.055 mg/kg), hydrocortisone (HC; 15 mg/kg), or MT-2 (1, 10, and 100 ng/kg). (*$P < 0.05$ versus Con, $n = 8$ per group). (**E**) Isometric tension of isolated tracheal spirals at baseline (control without challenge or treatment), challenged with acetylcholine without treatment (ACh) or treated with TB (1500 nM) or MT-2 (15, 30, and 60 nM) (*$P < 0.05$ versus ACh and $^{\#}P < 0.05$ versus TB, $n = 5$ per group). (**F**) Collagen gel contraction assays of rat airway smooth muscle cells (ASMCs) at baseline (control without treatment) or treated with TB (10,000 nM) or MT-2 (15, 30, and 60 nM) (*$P < 0.05$ versus baseline, $n = 3$ per group). (**G**) Real-time cell analysis of rat ASMCs at baseline (control without challenge or treatment), challenged with acetylcholine without treatment (ACh) or treated with TB (10,000 nM) or MT-2 (60 nM) (*$P < 0.05$ versus ACh and $^{\#}P < 0.05$ versus TB, $n = 4$ per group). All data are expressed as means ± SEM. Statistical analyses were performed by one-way analysis of variance (ANOVA) with the Games-Howell/least significant difference (LSD) post hoc test.

Downloaded from http://stm.sciencemag.org/ by guest on July 7, 2021

MT-2 binds to TG2 in ASMCs

To identify the MT-2 receptors relaxing ASMCs after treatment, we first synthesized fluorescein isothiocyanate (FITC)–conjugated recombinant MT-2 protein for confocal microscopy (fig. S2A). FITC–MT-2 bound to the membrane of live rat ASMCs as confirmed by 95% colocalization with DiI stain [$DiIC_{18}(3)$], a typical marker for the cellular membrane (Fig. 2A). We then used ^{125}I-labeled MT-2 (^{125}I–MT-2) to analyze the binding of MT-2 to ASMCs. MT-2 showed a strong and linear Scatchard plot of binding to ASMCs, showing that this interaction is mediated by a single receptor. We also confirmed that this was a strong interaction with a 33.4 nM K_D (equilibrium dissociation constant), 6.6×10^5 surface binding sites per cell, and 110 pM B_{max} (maximum combined value; Fig. 2B). All these results suggest the existence of a single MT-2 receptor relaxing ASMCs.

We next identified the MT-2–binding proteins on ASMCs. First, we used 6×His tag MT-2 recombinant protein as a probe to incubate ASMCs membrane lysates and pull-down potential receptors. The pull-down extracts showed two bands of 30 and 50 kDa that were recognized by both anti-His and anti–MT-2 antibodies (Fig. 2C). Mass spectrometer analyses of the 30-kDa band matched TG2, and the 50-kDa band matched enolase-1 ($\Delta Cn \geq 0.1$ and $Xcorr \geq 3.75$; fig. S2, B and C). Then, we analyzed the role of both proteins in competitive binding experiments using blocking antibodies. ASMCs were incubated with blocking antibodies against TG2 enolase-1, D2 subclass of dopamine receptor (D2DR) as a negative control, and bovine serum albumin (BSA). ^{125}I–MT-2 (0.2 nM) was used as a hot probe to quantify the specific binding, and the competitive binding assays were performed with cold nonlabeled probe of MT-2 at 50×, 100×, and 250× excess. Cold MT-2 protein inhibited the binding of ^{125}I–MT-2 to ASMCs in a concentration-dependent manner (Fig. 2D). The binding of ^{125}I–MT-2 to ASMCs was inhibited only with the anti-TG2 antibody and was not affected by any of the other antibodies against enolase-1, D2DR, or BSA (Fig. 2D).

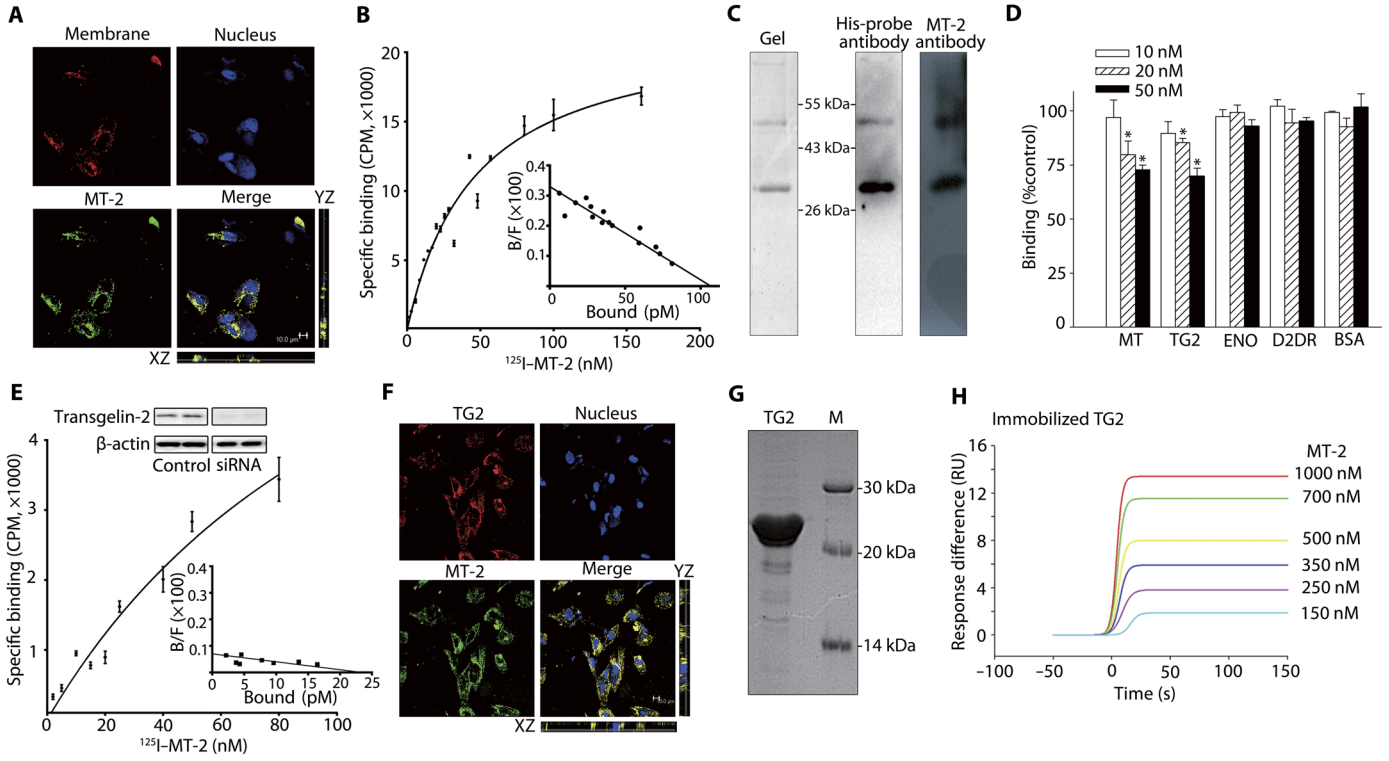

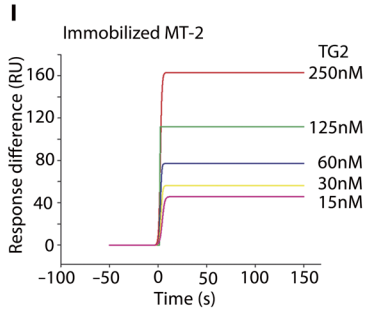

Fig. 2. MT-2 relaxes ASMCs specifically via transgelin-2. (**A**) Confocal images of rat ASMCs showing the cellular membrane [$DiIC_{18}(3)$, red], nucleus (Hoechst, blue), and MT-2 [FITC (fluorescein isothiocyanate), green] (scale bar, 10.0 μm). (**B**) Scatchard analysis of the binding of MT-2 to rat ASMCs ($n = 3$ per concentration). CPM, counts per minute. (**C**) Gel and Western blots using anti-His or anti–MT-2 antibody of immunoprecipitates of rat ASMCs lysates incubated with nickel–nitrilotriacetic acid beads linked to 6×His tag MT-2 recombinant protein used as a probe. (**D**) The competitive binding assays were performed with nonlabeled cold MT-2 (MT) or blocking antibodies against transgelin-2 (TG2), enolase-1 (ENO), D2 subclass of dopamine receptor (D2DR), or bovine serum albumin (BSA), whereas ^{125}I–MT-2 was used to quantify the specific binding of MT-2 to rat ASMCs (*$P < 0.05$ versus control without treatment, $n = 3$ per group). (**E**) Western blots of TG2 and β-actin of rat ASMCs treated with control or TG2 small interfering RNA (siRNA). Lower panel: Scatchard analysis of the binding of MT-2 to TG2-deficient rat ASMCs ($n = 3$ per concentration). (**F**) Confocal images of rat ASMCs showing TG2 (TG2, Cy3; red), nucleus (Hoechst, blue), and MT-2 (FITC, green) (scale bar, 10.0 μm). (**G**) Gel of purified rat recombinant TG2 protein and molecular weight markers (M). (**H**) Kinetic analysis of MT-2 by Biacore surface plasmon resonance with TG2 immobilized on the CM5 sensor chip. RU, response units. (**I**) Kinetic analysis of TG2 in Biacore surface plasmon resonance with MT-2 immobilized on the CM5 sensor chip. The response signals were recorded over the indicated time periods. All data are expressed as means ± SEM. Statistical analyses were performed by one-way ANOVA with the Games-Howell/LSD post hoc test.

Downloaded from http://stm.sciencemag.org/ by guest on July 7, 2021

The specific binding of MT-2 to TG2 was confirmed by inhibiting TG2 expression in ASMCs. First, the efficacy of small interfering RNA (siRNA) to inhibit TG2 expression was confirmed by Western blot analyses (Fig. 2E). Inhibition of TG2 expression specifically inhibited the B_{max} of ^{125}I–MT-2 binding to ASMCs by more than 80% without affecting the K_D (Fig. 2E). By contrast, inhibition of enolase-1 expression did not affect the B_{max} of MT-2 binding to ASMCs (fig. S2D). Next, we studied the colocalization of MT-2 and TG2 on ASMCs by confocal microscopy. The images showed a strong signal of MT-2 at the membrane of live rat ASMCs and more than 95% colocalization with TG2 (Fig. 2F).

The binding of MT-2 to TG2 was then studied at the structural level. MT-2 and TG2 were purified by affinity chromatography in Ni-NTA columns (Fig. 2G). Their interaction was studied with Biacore surface plasmon resonance showing a strong interaction between MT-2 and TG2. MT-2 binds to TG2 linked to the CM5 sensor chip with a K_D of 442 nM (Fig. 2H). Conversely, TG2 binds to MT-2 linked to the sensor chip with a K_D of 110 nM (Fig. 2I). To study the structural domain of MT-2 binding to TG2, we analyzed the binding of the truncated α or β MT-2 domains to TG2. Neither the truncated α nor the β MT-2 domain fragment bound to TG2 by itself (fig. S2, E and F). These results suggest that both domains contribute to MT-2 binding to TG2. The findings from these various assays concur in showing that MT-2 specifically binds to TG2 on the membrane of ASMCs.

MT-2 relaxes ASMCs via TG2

We inhibited TG2 expression to determine whether it is specifically required for MT-2 to relax ASMCs. The specific inhibition of TG2 protein expression by siRNA was confirmed by Western blotting. TG2 inhibition prevented the potential of MT-2 to reduce rat ASMCs contraction induced by either collagen or acetylcholine (Fig. 3, A and B). Then, we reasoned that inhibition of TG2 would render the animals more susceptible to asthma similar to the results described in MT-KO mice. Thus, we generated the TG2 knockout (TG2-KO) mice and confirmed TG2 inhibition by polymerase chain reaction (PCR) and Western blotting (fig. S3 and Fig. 3C). As anticipated, TG2-KO mice were more susceptible to asthma and had about twofold higher pulmonary resistance than control mice (Fig. 3D).

The binding of MT-2 to TG2 may have a potential biological function in asthma because transgelins are actin-binding proteins that relax the cellular cytoskeleton. Thus, we analyzed the MT-2/TG2 intracellular mechanism relaxing ASMCs by using a protein antibody array. Of 1318 proteins involved in more than 30 cellular pathways analyzed, the most significant effects of MT-2 were to induce the phosphorylation of ezrin and the dephosphorylation of myosin phosphatase target subunit 1 (MYPT1). These results were confirmed by Western blots against the phosphorylated isoforms compared to the total protein (Fig. 3E). Ezrin was the cytoskeletal protein with the most significant induction of phosphorylation as confirmed

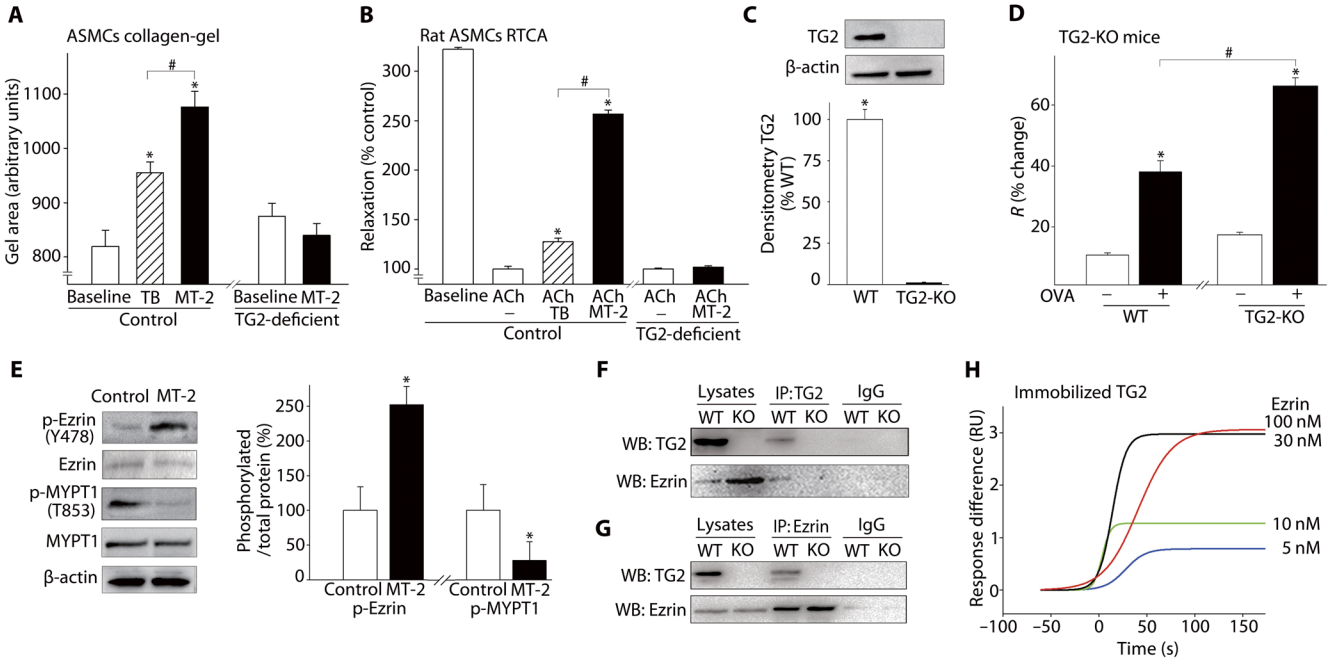

Fig. 3. Biological function of TG2 and the interaction with MT-2. (**A**) Collagen gel contraction assays of rat ASMCs at baseline (control without treatment) or treated with TB (10,000 nM) or MT-2 (60 nM) (*$P < 0.05$ versus baseline and #$P < 0.05$ versus TB, $n = 3$ per group). (**B**) Comparison of control and TG2-deficient rat ASMCs challenged with acetylcholine without treatment (ACh) or treated with TB (10,000 nM) or MT-2 (60 nM) (*$P < 0.05$ versus ACh and #$P < 0.05$ versus TB, $n = 4$ per group). (**C**) Western blot analyses of TG2 and β-actin in lung tissue from WT or TG2 knockout (TG2-KO) mice. Lower panel: Mean density of TG2 protein normalized to β-actin protein (*$P < 0.05$ versus TG2-KO by t test, $n = 3$ per group). (**D**) Pulmonary resistance (R) in WT and TG2-KO mice sensitized to OVA and challenged with vehicle (control) or OVA. (*$P < 0.05$ versus control and #$P < 0.05$ versus WT mice challenged with OVA, $n = 8$ per group). (**E**) Western blot analyses of MT-2 on the phosphorylation and total protein of ezrin, myosin phosphatase target subunit 1 (MYPT1) in rat ASMCs. Right panel: Corresponding densitometric analyses showing phosphorylated/total protein (%) treated with vehicle (control) or MT-2 (30 nM) (*$P < 0.05$ versus control, t test; $n = 3$ per group). (**F**) Western blots of TG2 and ezrin in total lysates or immunoprecipitates with TG2 antibody (IP: TG2) or control immunoglobulin G (IgG) of lung tissue from WT or TG2-KO mice. (**G**) Western blots of TG2 and ezrin in total lysates or immunoprecipitates with ezrin antibody (IP: Ezrin) or control IgG of lung tissue from WT or TG2-KO mice. (**H**) Kinetic analysis of ezrin by Biacore surface plasmon resonance with TG2 immobilized on the CM5 sensor chip. The response signals were recorded over the indicated time periods. All data are expressed as means ± SEM. Statistical analyses were performed by one-way ANOVA with the Games-Howell/LSD post hoc test.

Downloaded from http://stm.sciencemag.org/ by guest on July 7, 2021

by Western blotting and the only protein that coimmunoprecipitated with TG2 (Fig. 3, F and G). Previous studies showed that ezrin is a structural protein involved in stabilizing membrane receptor complexes (*26*, *27*). We reasoned that ezrin may interact with TG2 to stabilize the membrane receptor complex. Thus, we analyzed whether ezrin binds to TG2 by coimmunoprecipitating either ezrin or TG2. Both anti-TG2 coimmunoprecipitated ezrin in mouse lung tissue and, conversely, anti-ezrin coimmunoprecipitated TG2 (Fig. 3, F and G). These interactions were specific because they did not appear in the control immunoglobulin G immunoprecipitates. We next confirmed the direct TG2-ezrin interaction with Biacore surface plasmon resonance. TG2 and ezrin showed a strong interaction with a K_D of 73.3 nM with TG2 covalently linked to the CM5 sensor chip (Fig. 3H). These results concur with previous studies showing that ezrin is a critical structural protein orchestrating receptor complexes and their interaction with the actin cytoskeleton (*26*). Thus, ezrin may play a critical role in regulating TG2 localization and interaction with the actin cytoskeleton.

TSG12 is a specific TG2 agonist in ASMCs

We reasoned that TG2 agonists may control pulmonary resistance in asthma. To identify specific TG2 agonists, we performed molecular docking analyses for more than 6000 compounds from an in-house database based on the nuclear magnetic resonance structure for the binding site of TG2 CH domain. Of these 6000 compounds, 21 showed an optimal docking score (<−6 Kcal/mol) (table S1), and each compound was analyzed biologically by surface plasmon resonance analyses. Among these, TSG12 ($C_{21}H_{21}N_3O_4S_3$, *N*-[4-[(8-methoxy-4,4-dimethyl-5*H*-dithiolo[3,4-c]quinolin-1-ylidene)amino]phenyl]sulfonylacetamide) showed the strongest interaction with TG2 with a K_D value of 11 nM (Fig. 4A). The docking study revealed that TG2 residues Lys^{57}, Gln^{89}, and Val^{42} could form hydrogen bonds with TSG12, and residues Asn^{54}, Trp^{55}, Lys^{57}, Asp^{58}, Thr^{60}, Ala^{82}, Ala^{86}, and Trp^{117} were predicted to have van der Waals interaction with TSG12 (Fig. 4B).

Next, we analyzed whether TSG12 relaxes ASMCs specifically via TG2. TSG12 specifically inhibited acetylcholine-induced rat ASMCs contraction in control but not in TG2-deficient ASMCs (Fig. 4C). TSG12 inhibited acetylcholine-induced rat ASMCs contraction in a dose-dependent manner with a half-maximal effective concentration (EC_{50}) of 6.8 nM. We then used TG2-KO mice to analyze the specificity of TSG12 in vivo. TSG12 reduced asthmatic pulmonary resistance in control but not in TG2-KO asthmatic mice (Fig. 4D). Next, we studied whether TSG12 induced immunological effects by analyzing cell and immune cytokines in the bronchoalveolar lavage fluid (BALF). Asthmatic mice challenged with house dust mite (HDM) were treated with TSG12 (100 ng/kg), and the BALF was analyzed. TSG12 did not affect the percentages of lymphocytes, neutrophils, or eosinophils (table S2). Likewise, TSG12 did not affect the inflammatory cytokines analyzed [interleukin-2 (IL-2), IL-4, IL-5, or IL-13; table S2]. There were no significant correlations between pulmonary resistance of TSG12 treatment and the percentages of lymphocytes, neutrophils, and eosinophils or levels of IL-2, IL-4, IL-5, and IL-13 (table S3). These results showed the specificity of TSG12 both in vivo and in vitro and that TSG12 did not induce significant immunological effects in the BALF.

Given that TSG12 relaxed ASMCs, we analyzed whether it also affects the vascular smooth muscles. We analyzed the effects of TSG12 inhalation on blood pressure in vivo by using tail-cuff plethysmography as previously reported (*28*, *29*). Isoproterenol inhalation (10 μg/kg) increased systolic blood pressure (111.6 ± 1.9 mmHg versus 137.5 ± 10.6 mmHg; $P < 0.05$; $n = 8$), but TSG12 inhalation (10 μg/kg) did not affect blood pressure (119.8 ± 2.8 mmHg versus 120.6 ± 4.1 mmHg; $P > 0.05$; $n = 8$). Then, we analyzed TSG12 distribution after inhalation in the serum and organs by liquid chromatography–electrospray ionization tandem mass spectrometry (*30*). TSG12 accumulated in the trachea and lung (Fig. 4E). Only small traces of TSG12 were observed in the blood, and TSG12 was not detected in the other organs (Fig. 4E). We next analyzed the metabolic stability of TSG12 and determined that the half-life ($t_{1/2}$) of TSG12 was 74.1, 13.7, and 37 min in human, mouse, and rat liver microsomes, respectively (table S4). These results show that TSG12 is a stable compound in vivo. We analyzed whether TSG12 affects pulmonary arteries by using precision-cut lung slices. Lung slices sectioning arteries with the lumen surrounded with smooth muscle cells identified as "dark rings" (*31*) and airways with the lumen lined by epithelial cells with ciliary activity (*32*) were treated with TSG12 for 10 min and compared to control treatments. As expected, potassium chloride and sodium nitroprusside contracted and dilated the artery cross-sectional areas, respectively (Fig. 4F). By contrast, TSG12 (0.1 μM) did not affect the arteries (Fig. 4F), but it relaxed the airways twofold more effectively than 100 μM isoproterenol (Fig. 4G).

Next, we analyzed the intracellular mechanism of TSG12. First, we confirmed that TSG12 treatment induced MYPT1 dephosphorylation at Thr^{853} in rat tracheal spirals similar to that described above for MT-2 (Fig. 4H). Then, we confirmed that TSG12 induced the dephosphorylation of both MYPT1 and MLC in ASMCs (Fig. 4I). Given that unphosphorylated MYPT1 at Thr^{853} activates the myosin light-chain phosphatase (MLCP) complex to dephosphorylate MLC and induces muscle relaxation, these results indicate that TSG12 activated MYPT1 to dephosphorylate MLC and thereby induced ASMCs relaxation. Then, we analyzed the effects of TSG12 on the RhoA-ROCK-MYPT1-MLC pathway to determine whether TSG12 regulated MYPT1/MLC through this pathway or whether this was a collateral effect induced by another pathway. TSG12 induced ROCK dephosphorylation at Tyr^{722} and RhoA phosphorylation at Ser^{188} (Fig. 4I). Given that this phosphorylation inhibits RhoA and prevents ROCK phosphorylation, our results suggest that TSG12 regulates the RhoA-ROCK-MYPT1-MLC pathway by inhibiting RhoA and hence inducing MLC dephosphorylation and relaxing ASMCs.

TG2 agonist TSG12 relaxes ASMCs and abrogates pulmonary resistance in asthma

We analyzed the effects of TSG12 in two experimental models of asthma, including mice challenged with either OVA or HDM. HDM is also a common allergen with major clinical implications, causing human allergic asthma (*33*). TSG12 inhalation significantly inhibited pulmonary resistance in mice challenged with OVA in a concentration-dependent manner ($P < 0.05$; Fig. 5A). In vivo, TSG12 was more effective than conventional β_2-agonist terbutaline in inhibiting pulmonary resistance. Likewise, TSG12 also inhibited pulmonary resistance by more than 80% in mice with HDM asthma (Fig. 5B). Again, TSG12 was more effective than the β-agonist isoproterenol in reducing pulmonary resistance in HDM asthma. As an additional control, we used inactive control compound (CC) with a similar chemical structure of TSG12 but without biological activity because it lacks the active carbonyl group (fig. S4A).

Then, we analyzed the clinical potential of TSG12 to relax human ASMCs. First, we confirmed that TSG12 is not cytotoxic to human ASMCs as shown by cell viability assay (fig. S4B). Then, we analyzed

Downloaded from http://stm.sciencemag.org/ by guest on July 7, 2021

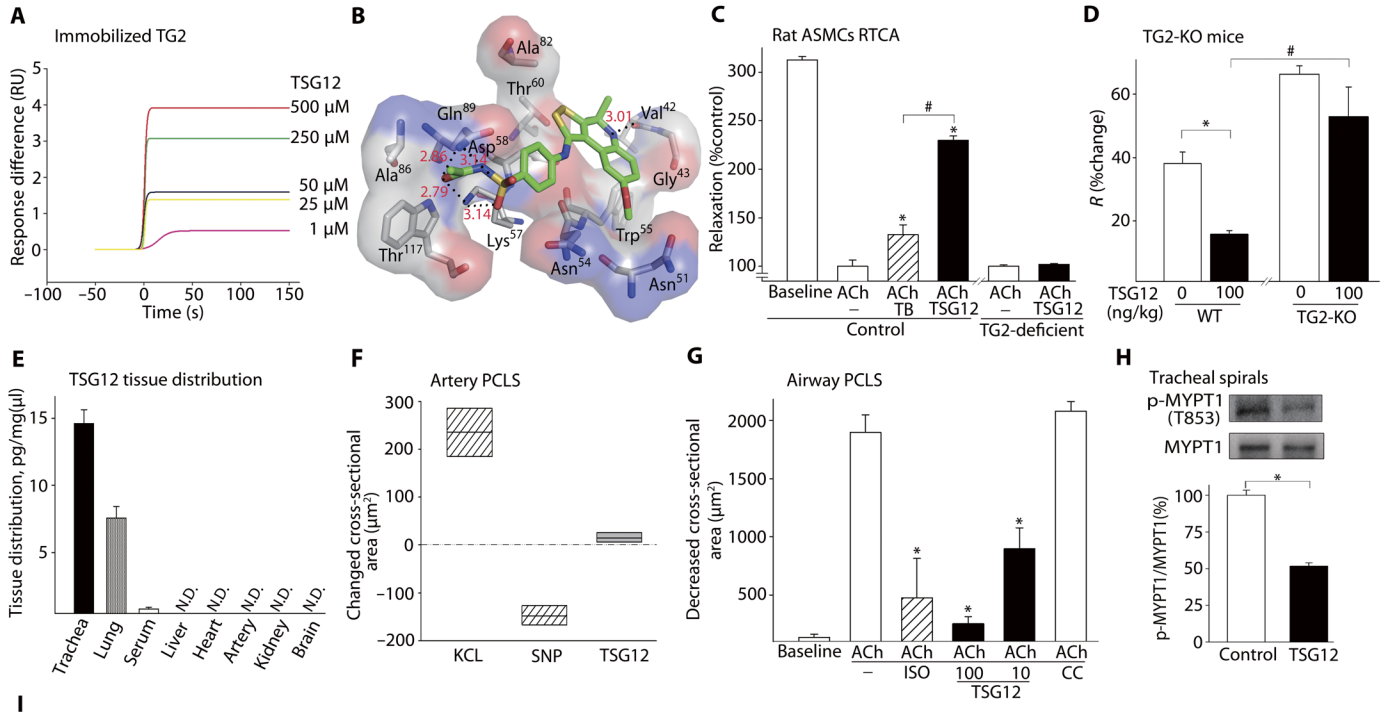

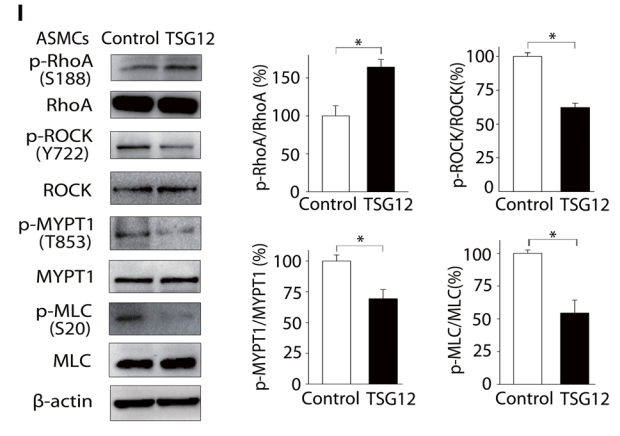

Fig. 4. TSG12 is a specific TG2 agonist in ASMCs. (**A**) Kinetic analysis of TSG12 by Biacore surface plasmon resonance with TG2 immobilized on the CM5 sensor chip. The response signals were recorded for the indicated time. (**B**) Schematic interaction of the molecular docking of TSG12 and TG2 (Protein Data Bank code: 1WYM). (**C**) Comparison of control and TG2-deficient rat ASMCs challenged with acetylcholine without treatment (ACh) or treated with TB (10,000 nM) or TSG12 (50 nM) (*$P < 0.05$ versus ACh and #$P < 0.05$ versus TB, $n = 4$ per group). (**D**) Pulmonary resistance (R) in OVA-induced asthma WT and TG2-KO mice treated with vehicle (control) or TSG12 (100 ng/kg). (*$P < 0.05$ versus control and #$P < 0.05$ versus WT mice treated with TSG12, $n = 8$ per group). (**E**) TSG12 organ and serum distribution after inhalation. The distribution of TSG12 in different tissues after inhalation of TSG12 in mice ($n = 3$ per group) was determined by liquid chromatography–electrospray ionization tandem mass spectrometry and expressed as picograms per milligram of tissue or picograms per microliter of serum. N.D. means not detected or the concentration is lower than the limit of detection (0.1 pg/mg tissue). (**F**) The changed cross-sectional area (μm^2) in precision-cut lung slices (PCLS) of arteries incubated with potassium chloride (KCL, 150 mM), sodium nitroprusside (SNP, 100 μM), or TSG12 (100 nM; $n = 4$ per group). (**G**) Decreased cross-sectional area (μm^2) in PCLS of airways challenged with acetylcholine without treatment (ACh) or treated with isoproterenol (ISO; 100 μM); TSG12 (10 and 100 nM) or inactive control compound (CC; 100 nM). (*$P < 0.05$ versus ACh, $n = 4$ per group). (**H**) Western blot analyses of TSG12 on the phosphorylation and total protein of MYPT1 in rat tracheal spirals. Lower panel: Corresponding densitometric analyses showing phosphorylated/total protein (%) treated with vehicle (control) or TSG12 (25 μM). (*$P < 0.05$ versus control, t test; $n = 3$ per group). (**I**) Western blot analyses of TSG12 on the phosphorylation and total protein of RhoA, ROCK, MYPT1, and myosin light chain (MLC) in murine ASMCs. Right panels: Corresponding densitometric analyses showing phosphorylated/total protein (%) treated with vehicle (control) or TSG12 (25 μM). (*$P < 0.05$ versus control, t test; $n = 3$ per group). All data are expressed as means ± SEM. Statistical analyses were performed by one-way ANOVA with the Games-Howell/LSD post hoc test.

the effects of TSG12 on human ASMCs using real-time cell analysis (RTCA), optical magnetic twisting cytometry (OMTC), and traction force microscopy (TFM) assays (Fig. 5, C to F). TSG12 relaxed human ASMCs in a dose-dependent manner with an EC_{50} of 5.2 nM. Again, this effect was specific because TSG12 relaxed control but not TG2-deficient human ASMCs generated by RNA interference (Fig. 5C). TSG12 significantly reduced the acetylcholine-induced contraction of human ASMCs by more than 80% as shown by OMTC ($P < 0.05$; Fig. 5D). TSG12 also decreased the traction force of human ASMCs (Fig. 5, E and F), whereas cell-projected areas were not different among groups (fig. S4C). Together, these results show the potential of TSG12 to control pulmonary resistance in different models of asthma in vivo and to relax human ASMCs.

We next analyzed whether TSG12 induces TG2 receptor desensitization. One limitation of β-agonists is that they cause adrenoceptor desensitization, leaving the patients unresponsive with uncontrolled symptoms. We previously observed that β_2-agonists, such as salbutamol, induced a quick but temporal relaxation of human ASMCs. Then, the cells became insensitive to a second treatment for over a day, without an alternative therapeutic treatment to relax ASMCs (*34*). However, β_2-adrenoceptor desensitization did not affect TSG12 potential to relax ASMCs. Human ASMCs treated with salbutamol lose initial response to a second treatment with β_2-agonist. However, these cells are still responsive to 10 nM TSG12 (Fig. 5G). TSG12 inhibited the acetylcholine-induced contraction of human ASMCs regardless of the β_2-adrenoceptor desensitization (Fig. 5G). Treatment

Downloaded from http://stm.sciencemag.org/ by guest on July 7, 2021

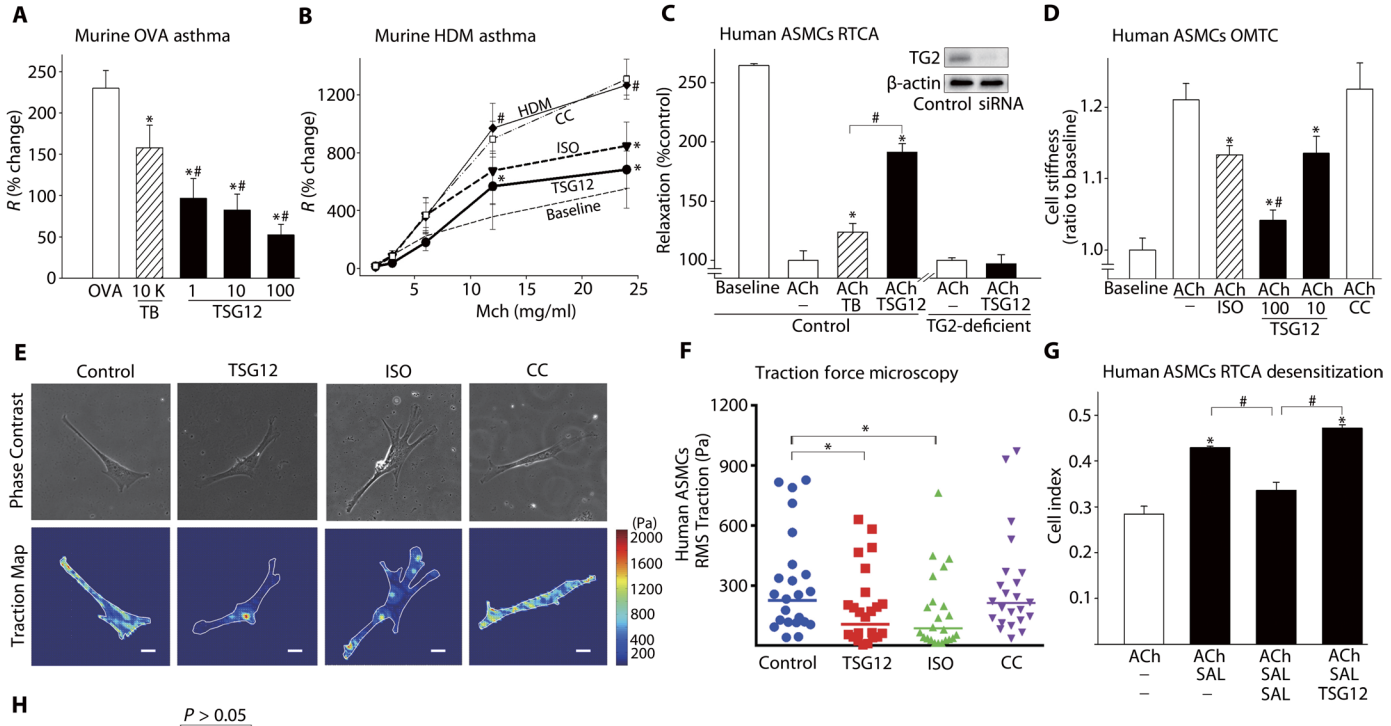

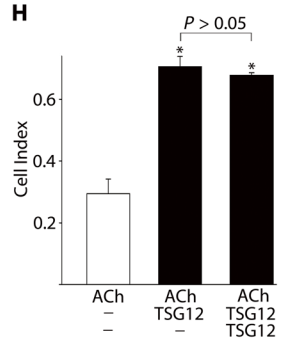

Fig. 5. TG2 agonist TSG12 relaxes ASMCs and ameliorates pulmonary resistance. (**A**) Pulmonary resistance (*R*) in OVA-challenged mice treated with vehicle (OVA), TB, or TSG12 (*$P < 0.05$ versus OVA and #$P < 0.05$ versus TB, $n = 15$ per group). (**B**) Pulmonary resistance (*R*) at baseline [control without house dust mite (HDM)] and HDM-challenged mice treated with vehicle (HDM), ISO (10 μg/kg), or TSG12 (100 ng/kg) or inactive CC (100 ng/kg). (*$P < 0.05$ versus HDM and #$P < 0.05$ versus baseline, $n = 8$ per group). Mch, methacholine. (**C**) Western blot analyses of TG2 (TG2) and β-actin in human ASMCs treated with control or specific siRNA inhibiting TG2 expression. Lower panel: Real-time cell analysis of control and TG2-deficient human ASMCs challenged with acetylcholine without treatment (ACh) or treated with TB (10,000 nM) or TSG12 (50 nM). (*$P < 0.05$ versus ACh and #$P < 0.05$ versus TB, $n = 4$ per group). (**D**) Optical magnetic twisting cytometry of human ASMCs challenged with acetylcholine without treatment (ACh) or with ISO (100 μM), TSG12 (10 and 100 nM) or, inactive CC (100 nM). (*$P < 0.05$ versus ACh and #$P < 0.05$ versus ISO, $n = 4$ per group). (**E**) Phase-contrast images and traction maps of human ASMCs (scale bars, 20.0 μm). (**F**) Traction force of human ASMCs treated with vehicle (control) or treated with TSG12 (100 nM), ISO (100 μM), or inactive CC (100 nM). Bars are the geometric means of the respective group. Cell traction data are converted to log scale before the statistical analyses. (*$P < 0.05$ versus control, $n = 23$ per group). (**G**) Real-time cell analysis of human ASMCs challenged with acetylcholine without treatment (ACh) or treated with salbutamol (SAL; 10 μM) or with a second treatment of either salbutamol (SAL/SAL; 10 μM) or TSG12 (SAL/TSG12; 10 nM) within 24 hours. (*$P < 0.05$ versus ACh and #$P < 0.05$ versus human ASMCs with β_2-adrenoceptor desensitization, $n = 4$per group). (**H**) Real-time cell analysis of human ASMCs challenged with acetylcholine without treatment (ACh) or treated with TSG12 (10 nM) or with a second treatment (TSG12/TSG12; 10 nM) within 24 hours (*$P < 0.05$ versus ACh, $n = 4$ per group). All data are expressed as means ± SEM. Statistical analyses were performed by one-way ANOVA with the Games-Howell/LSD post hoc test.

with TSG12 relaxed human ASMCs without inducing receptor desensitization, and a second TSG12 treatment within 24 hours still relaxed human ASMCs with similar efficacy (Fig. 5H). These results indicate that TSG12 relaxed human ASMCs specifically via TG2 without inducing receptor desensitization and losing its efficacy.

DISCUSSION

Our study shows that inhibition of MT-2 protein expression contributes to pulmonary resistance in asthma. Although metallothioneins protect against pulmonary oxidative stress during endotoxemia (*23*), they have not been studied in asthma. Here, we show the inhibition of MT-2 protein expression in asthmatic lung tissue and that MT-2 inhibition increases pulmonary resistance in asthma. Conversely, treatment with recombinant MT-2 reduces the isometric tension of isolated tracheal spirals. This effect is not challenge-specific, because MT-2 reduces ASMCs contraction induced by either acetylcholine or collagen. In vivo, treatment with recombinant MT-2 was more effective than conventional treatment with β_2-agonists or corticosteroid in reducing pulmonary resistance in asthmatic rats. Together, these results support MT-2 as a physiological regulator of ASMCs modulating pulmonary resistance.

All our experiments show that MT-2 binds to and relaxes ASMCs specifically via TG2. TG2 is an abundant protein in smooth muscle cells and a member of the calponin protein family (*35*). Several studies have indicated the role of TG2 as a membrane protein that increased actin stability at the immunological synapse (*36*, *37*). The transgelin-homolog Scp1 protein is a component of yeast cortical actin patches (*36*), and TG2 is present in the membrane of radial lamellipodium T cells, accumulates in the filopodia of B cell immunological synapses (*37*, *38*), and localizes at the membrane ruffles of lipopolysaccharide-stimulated macrophages (*39*). TG2 can also regulate the cytoskeleton of endothelial cells, and lovastatin induces TG2 expression to inhibit human umbilical vein endothelial cell migration and tube formation (*40*). These results for TG2 are reminiscent of previous studies of enolase-1. Enolase-1 was first described as an intracellular key

Downloaded from http://stm.sciencemag.org/ by guest on July 7, 2021

glycolytic enzyme and was later proved to serve as a plasminogen membrane receptor on the surface of hematopoietic, epithelial, and endothelial cells (*41*). Likewise, TG2 was originally described as a critical regulator of the actin cytoskeleton. Now, our study concurs with growing evidence, indicating that TG2 is a membrane component that regulates the cytoskeleton in response to extracellular signals, such as MT-2.

In addition to the binding studies, we also analyzed that TG2 specifically mediates MT-2–induced ASMCs relaxation both in vitro and in vivo. In vitro, MT-2 relaxes control but not TG2-deficient ASMCs. Then, we generated TG2-KO mice and observed that TG2 gene deletion increased pulmonary resistance in asthma. The intracellular mechanism of TG2 to relax ASMCs was analyzed by protein array analyses of more than 30 pathways. The most significant effects of TG2 activation with MT-2 were the phosphorylation of ezrin and the dephosphorylation of MYPT1. MT-2 binding to TG2 induces the phosphorylation of ezrin, which is a structural protein that stabilizes transmembrane receptor complexes with the cytoskeleton (*42*). Ezrin was the only protein that coimmunoprecipitated with TG2, and it was also the protein in the cytoskeletal pathway that showed the most significant induction of phosphorylation. Ezrin is a principal member of the ERM (ezrin-radixin-moesin) family encompassed by actin-binding proteins with an N terminus similar to that of the erythrocyte cytoskeletal protein band 4.1 (*43*). Ezrin is a critical structural protein that orchestrates receptor complexes, their signaling pathways, and interaction with the cytoskeleton (*26*, *42*). TG2 is a relatively small protein that requires structural intracellular proteins for its signal transduction. Thus, ezrin may play a critical role in regulating TG2 localization, its signaling pathways, and interactions with the cytoskeleton. This interaction is similar to the binding of CD44 to ezrin and other ERM proteins during the cytoskeletal reorganization in cell-cell adhesion and migration (*44*). TG2 coimmunoprecipitates with ezrin, and the Biacore surface plasmon resonance study confirmed that ezrin and TG2 had a strong interaction with a K_D of 73.3 nM. These results indicate that ezrin associates with TG2 to stabilize the membrane receptor complex. On the other hand, TG2 dephosphorylates MYPT1 Thr^{853} and thereby relaxes ASMCs. Unphosphorylated Thr^{853} MYPT1 is a critical regulator that joins M20 and protein phosphatase 1Cδ to form the active MLCP complex, which dephosphorylates MLC and relaxes ASMCs (*45*, *46*). These results show that MT-2 relaxes ASMCs via TG2 and induces MYPT1 dephosphorylation. Our results support TG2 as a link between extracellular signals (MT-2) and both actin and myosin cytoskeletons in ASMCs via ezrin and MYPT1, respectively.

Although all our experiments in vitro and in vivo show that MT-2 binds to and relaxes ASMCs specifically via TG2, our pull-down experiments also reveal the potential binding of MT-2 to enolase-1 in vitro. Although we did not find any evidence of this interaction in vivo, our results do not rule out the possibility that MT-2 binding to enolase-1 may have biological implications. Enolase-1 is a key glycolytic enzyme that can also serve as a plasminogen receptor on the surface of hematopoietic, epithelial, and endothelial cells (*41*), but it has not been reported in muscle cells. Thus, enolase-1 might represent an alternative MT-2 receptor in other cell types (*47*) or a secreted enzyme that binds to extracellular MT-2 (*48*). Our results suggest that MT-2 can be more effective injected intravenously for reducing pulmonary resistance in vivo than when using ex vivo on tracheal spirals. The mechanisms of airway constriction in vivo are not linear with those of ASMCs contraction in vitro, and many factors affect intravenous treatment of pulmonary resistance in vivo compared to the ex vivo treatment of tracheal spirals. To avoid potential side effects, we focused our efforts on identifying specific agonists for TG2 and analyzing their potential for treating asthma.

The role of TG2 mediating MT-2–induced relaxation of asthmatic pulmonary resistance suggests that this receptor can be a promising therapeutic target for asthma. We identified TSG12 as a specific TG2 agonist with potential therapeutic advantages in asthma, and the specificity of TSG12 for TG2 was confirmed both in vitro and in vivo.

The intracellular mechanism studies indicated that TSG12 induced MYPT1 dephosphorylation in rat tracheal spirals similar to that described above for MT-2. TSG12 induced the dephosphorylation of both MYPT1 and MLC in ASMCs, which is likely what led to ASMCs relaxation. Then, we analyzed the effects of TSG12 on the upstream pathway. TSG12 induced ROCK dephosphorylation at Tyr^{722} and RhoA phosphorylation at Ser^{188}. Given that the phosphorylation of Ser^{188} inhibits RhoA and prevents ROCK phosphorylation, our results show that TSG12 regulates the RhoA-ROCK-MYPT1-MLC pathway by inhibiting RhoA and thereby inducing MLC dephosphorylation and relaxing ASMCs (fig. S5).

A significant result of our study is the efficacy of TSG12 compared with conventional FDA-approved treatments, such as β_2-agonists. TSG12 inhibited pulmonary resistance in both experimental models, and it was more effective than standard β_2-agonists terbutaline or isoproterenol for inhibiting pulmonary resistance in OVA or HDM asthmatic mice, respectively. In human ASMCs, TSG12 reduces the acetylcholine-induced contraction in a dose-dependent manner. Furthermore, TSG12 provides therapeutic advantages in asthma compared to β_2-agonists. One critical limitation of β_2-agonists is that they induce β_2-adrenoceptor desensitization, leaving patients unresponsive with persistent uncontrolled symptoms. One single treatment with β_2-agonist leaves human ASMCs unresponsive to a second treatment for over a day. By contrast, TSG12 is still effective, and a 1000-fold lower concentration of TSG12 relaxes human ASMCs regardless of the β_2-adrenoceptor desensitization. Furthermore, our results indicate that TG2 is a receptor that is more resistant to desensitization, and unlike β_2-agonists, TSG12 treatment does not limit the efficacy of a secondary treatment.

However, limitations of the study should also be considered. First, given that ezrin is phosphorylated by several kinases, including RhoA and Src, the specific molecular mechanism inducing ezrin phosphorylation by TG2 is still uncertain. Second, whether MT-2 binding to enolase-1 may induce other effects increasing its efficacy on pulmonary resistance remains speculative and will need to be determined.

In summary, our study shows that MT-2 reduces asthmatic pulmonary resistance via TG2 by inducing dephosphorylation of MYPT1. TSG12, a nontoxic, specific TG2 agonist, relaxes human ASMCs and inhibits pulmonary resistance in asthma. TSG12 is more effective than β_2-agonists for relaxing human ASMCs with potential clinical advantages. These results suggest that TG2 agonists could be a promising therapeutic approach for treating asthma.

MATERIALS AND METHODS

Study design

The purpose of this study is to elucidate the mechanism controlling ASMCs contraction and to identify specific therapeutic agents that can provide pharmacological benefits to ameliorate asthmatic pulmonary resistance. Our study tests whether the down-regulation of

Downloaded from http://stm.sciencemag.org/ by guest on July 7, 2021

MT-2 protein expression contributes to the pathogenesis of asthma. The role of MT-2 in asthma was analyzed with MT-KO mice. Our study also includes cellular models of human and rat ASMCs and ex vivo studies of isolated tracheal spirals. To identify potential receptors for MT-2 on ASMCs, pull-down assays, mass spectrometry analyses, ligand-binding assays, and confocal microscopy were applied. The role of the receptor TG2 was then analyzed using TG2-KO mice, inhibiting the expression in vitro (siRNA) and protein antibody array. We present structural analyses including the expression and purification of specific protein domains, Biacore surface plasmon resonance analyses, and molecular docking to identify specific agonists for TG2 able to ameliorate pulmonary resistance in asthma (induced by OVA or HDM). The specificity of the agonist was tested in wild-type and TG2 knockdown human and rat ASMCs, TG2-KO mice. We also analyzed TSG12 efficacy with OMTC, TFM, and antidesensitization capability compared with conventional approved β_2-agonists. Primary data are located in table S5.

Statistical analysis

All data are shown as means ± SEM. The number of animals per group in each experiment was determined on the basis of previous statistical analyses by our group. The statistical significance of two data sets was assessed by the two-tailed Student's *t* test. Statistical significance among three or more data sets was calculated using one-way analysis of variance (ANOVA) followed by a least significant difference or Games-Howell post hoc test (depending on the data and the hypothesis tested). Correlations were evaluated by Pearson's correlation coefficient (r). P values lower than 0.05 were considered significant.

SUPPLEMENTARY MATERIALS

www.sciencetranslationalmedicine.org/cgi/content/full/10/427/eaam8604/DC1
Materials and Methods
Fig. S1. The time-response curves of pulmonary resistance for different doses of MT-2.
Fig. S2. The identification of TG2 as a binding protein and the interaction between TG2 and domains of MT-2.
Fig. S3. PCR confirmation of TG2-KO mice.
Fig. S4. Chemical structure of inactive CC, cell viability assay of TSG12, and cell projected areas among groups by TFM.
Fig. S5. Proposed mechanism of ASMCs relaxation induced by TG2.
Table S1. Compounds selected for bioassay from molecular docking.
Table S2. Percentages of cells and levels of inflammatory cytokines (picograms per milliliter) in BALF after TSG12 treatment.
Table S3. Correlation coefficient of pulmonary resistance of TSG12 treatment and cell percentages or inflammatory cytokines.
Table S4. The metabolism of TSG12 in liver microsomes of human, mouse, and rat.
Table S5. Primary data.
References (*49–60*)

REFERENCES AND NOTES

1. Global Initiative for Asthma, Global Strategy for Asthma Management and Prevention (2017); available at www.ginasthma.org.
2. S. Croisant, Epidemiology of asthma: Prevalence and burden of disease. *Adv. Exp. Med. Biol.* **795**, 17–29 (2014).
3. S. B. L. Barnett, T. A. Nurmagambetov, Costs of asthma in the United States: 2002–2007. *J. Allergy Clin. Immunol.* **127**, 145–152 (2011).
4. F. D. Martinez, D. Vercelli, Asthma. *Lancet* **382**, 1360–1372 (2013).
5. J. V. Fahy, Type 2 inflammation in asthma—Present in most, absent in many. *Nat. Rev. Immunol.* **15**, 57–65 (2015).
6. S. E. Wenzel, Asthma phenotypes: The evolution from clinical to molecular approaches. *Nat. Med.* **18**, 716–725 (2012).
7. J. B. Bice, E. Leechawengwongs, A. Montanaro, Biologic targeted therapy in allergic asthma. *Ann. Allergy Asthma Immunol.* **112**, 108–115 (2014).
8. S. Zuyderduyn, M. B. Sukkar, A. Fust, S. Dhaliwal, J. K. Burgess, Treating asthma means treating airway smooth muscle cells. *Eur. Respir. J.* **32**, 265–274 (2008).
9. P. B. Noble, C. D. Pascoe, B. Lan, S. Ito, L. E. M. Kistemaker, A. L. Tatler, T. Pera, B. S. Brook, R. Gosens, A. R. West, Airway smooth muscle in asthma: Linking contraction and mechanotransduction to disease pathogenesis and remodelling. *Pulm. Pharmacol. Ther.* **29**, 96–107 (2014).
10. J. A. Hirota, T. T. B. Nguyen, D. Schaafsma, P. Sharma, T. Tran, Airway smooth muscle in asthma: Phenotype plasticity and function. *Pulm. Pharmacol. Ther.* **22**, 370–378 (2009).
11. M. L. Dowell, T. L. Lavoie, J. Solway, R. Krishnan, Airway smooth muscle: A potential target for asthma therapy. *Curr. Opin. Pulm. Med.* **20**, 66–72 (2014).
12. D. A. Deshpande, W. C. H. Wang, E. L. McIlmoyle, K. S. Robinett, R. M. Schillinger, S. S. An, J. S. K. Sham, S. B. Liggett, Bitter taste receptors on airway smooth muscle bronchodilate by localized calcium signaling and reverse obstruction. *Nat. Med.* **16**, 1299–1304 (2010).
13. R. B. Penn, Physiology. Calcilytics for asthma relief. *Science* **348**, 398–399 (2015).
14. S. P. Peters, C. A. Jones, T. Haselkorn, D. R. Mink, D. J. Valacer, S. T. Weiss, Real-world Evaluation of Asthma Control and Treatment (REACT): Findings from a national Web-based survey. *J. Allergy Clin. Immunol.* **119**, 1454–1461 (2007).
15. G. Pelaia, A. Vatrella, R. Maselli, The potential of biologics for the treatment of asthma. *Nat. Rev. Drug Discov.* **11**, 958–972 (2012).
16. C. A. Akdis, Therapies for allergic inflammation: Refining strategies to induce tolerance. *Nat. Med.* **18**, 736–749 (2012).
17. M. Cazzola, C. P. Page, L. Calzetta, M. G. Matera, Pharmacology and therapeutics of bronchodilators. *Pharmacol. Rev.* **64**, 450–504 (2012).
18. S. Suissa, A. Ariel, US Food and Drug Administration-mandated trials of long-acting β-agonists safety in asthma: Will we know the answer? *Chest* **143**, 1208–1213 (2013).
19. S. Navarro, D. A. Pickering, I. B. Ferreira, L. Jones, S. Ryan, S. Troy, A. Leech, P. J. Hotez, B. Zhan, T. Laha, R. Prentice, T. Sparwasser, J. Croese, C. R. Engwerda, J. W. Upham, V. Julia, P. R. Giacomin, A. Loukas, Hookworm recombinant protein promotes regulatory T cell responses that suppress experimental asthma. *Sci. Transl. Med.* **8**, 362ra143 (2016).
20. E. H. Bel, S. E. Wenzel, P. J. Thompson, C. M. Prazma, O. N. Keene, S. W. Yancey, H. G. Ortega, I. D. Pavord; SIRIUS Investigators, Oral glucocorticoid-sparing effect of mepolizumab in eosinophilic asthma. *N. Engl. J. Med.* **371**, 1189–1197 (2014).
21. H. L. Butcher, W. A. Kennette, O. Collins, R. K. Zalups, J. Koropatnick, Metallothionein mediates the level and activity of nuclear factor κB in murine fibroblasts. *J. Pharmacol. Exp. Ther.* **310**, 589–598 (2004).
22. J. Hidalgo, M. Aschner, P. Zatta, M. Vašák, Roles of the metallothionein family of proteins in the central nervous system. *Brain Res. Bull.* **55**, 133–145 (2001).
23. K.-i. Inoue, M. Satoh, Metallothionein as a therapeutic molecular target against human diseases. *Curr. Pharm. Biotechnol.* **14**, 391–393 (2013).
24. C. D. Klaassen, J. Liu, S. Choudhuri, Metallothionein: An intracellular protein to protect against cadmium toxicity. *Annu. Rev. Pharmacol. Toxicol.* **39**, 267–294 (1999).
25. L.-M. Yin, H.-Y. Li, Q.-H. Zhang, Y.-D. Xu, Y. Wang, Y.-L. Jiang, Y. Wei, Y.-Y. Liu, Y.-Q. Yang, Effects of S100A9 in a rat model of asthma and in isolated tracheal spirals. *Biochem. Biophys. Res. Commun.* **398**, 547–552 (2010).
26. L.-M. Yin, T.-T. Duan, L. Ulloa, Y.-Q. Yang, Ezrin orchestrates signal transduction in airway cells. *Rev. Physiol. Biochem. Pharmacol.* 10.1007/112_2017_4 (2017).
27. A. L. Neisch, R. G. Fehon, Ezrin, radixin and moesin: Key regulators of membrane-cortex interactions and signaling. *Curr. Opin. Cell Biol.* **23**, 377–382 (2011).
28. S.-K. Choi, M. Galán, M. Partyka, M. Trebak, S. Belmadani, K. Matrougui, Chronic inhibition of epidermal growth factor receptor tyrosine kinase and extracellular signal-regulated kinases 1 and 2 (ERK1/2) augments vascular response to limb ischemia in type 2 diabetic mice. *Am. J. Pathol.* **180**, 410–418 (2012).
29. Z. Xu, W. Li, J. Han, C. Zou, W. Huang, W. Yu, X. Shan, H. Lum, X. Li, G. Liang, Angiotensin II induces kidney inflammatory injury and fibrosis through binding to myeloid differentiation protein-2 (MD2). *Sci. Rep.* **7**, 44911 (2017).
30. H. Huang, Y. Yang, C. Lv, W. Chang, C. Peng, S. Wang, G. Ge, L. Han, W. Zhang, R. Liu, Pharmacokinetics and tissue distribution of five bufadienolides from the Shexiang Baoxin pill following oral administration to mice. *J. Ethnopharmacol.* **161**, 175–185 (2015).
31. R. Paddenberg, P. Mermer, A. Goldenberg, W. Kummer, Videomorphometric analysis of hypoxic pulmonary vasoconstriction of intra-pulmonary arteries using murine precision cut lung slices. *J. Vis. Exp.*, e50970 (2014).
32. A. Bergner, M. J. Sanderson, ATP stimulates Ca^{2+} oscillations and contraction in airway smooth muscle cells of mouse lung slices. *Am. J. Physiol. Lung Cell. Mol. Physiol.* **283**, L1271–L1279 (2002).
33. J. K. Peat, E. Tovey, B. G. Toelle, M. M. Haby, E. J. Gray, A. Mahmic, A. J. Woolcock, House dust mite allergens. A major risk factor for childhood asthma in Australia. *Am. J. Respir. Crit. Care Med.* **153**, 141–146 (1996).
34. S. Fogli, F. Stefanelli, A. Martelli, S. Daniele, L. Testai, V. Calderone, M. L. Trincavelli, C. Martini, M. C. Breschi, Protective effect of high-dose montelukast on salbutamol-induced homologous desensitisation in airway smooth muscle. *Pulm. Pharmacol. Ther.* **26**, 693–699 (2013).

Downloaded from http://stm.sciencemag.org/ by guest on July 7, 2021

35. D. Rao, B. F. Kimler, W. B. Nothnick, M. K. Davis, F. Fan, O. Tawfik, Transgelin: A potentially useful diagnostic marker differentially expressed in triple-negative and non–triple-negative breast cancers. *Hum. Pathol.* **46**, 876–883 (2015).
36. A. Goodman, B. L. Goode, P. Matsudaira, G. R. Fink, The *Saccharomyces cerevisiae* calponin/transgelin homolog Scp1 functions with fimbrin to regulate stability and organization of the actin cytoskeleton. *Mol. Biol. Cell* **14**, 2617–2629 (2003).
37. B.-R. Na, H.-R. Kim, I. Piragyte, H.-M. Oh, M.-S. Kwon, U. Akber, H.-S. Lee, D.-S. Park, W. K. Song, Z.-Y. Park, S.-H. Im, M.-C. Rho, Y.-M. Hyun, M. Kim, C.-D. Jun, TAGLN2 regulates T cell activation by stabilizing the actin cytoskeleton at the immunological synapse. *J. Cell Biol.* **209**, 143–162 (2015).
38. B.-R. Na, M.-S. Kwon, M.-W. Chae, H.-R. Kim, C.-H. Kim, C.-D. Jun, Z.-Y. Park, Transgelin-2 in B-cells controls T-cell activation by stabilizing T cell - B cell conjugates. *PLOS ONE* **11**, e0156429 (2016).
39. C.-D. Jun, H.-R. Kim, Transgelin-2 mimics bacterial SipA and promotes membrane ruffling and phagocytosis in lipopolysaccharide-activated macrophages. *J. Immunol.* **196**, 63.15 (2016).
40. Y. Xiao, Y. Li, J. Han, Y. Pan, L. Tie, X. Li, Transgelin 2 participates in lovastatin-induced anti-angiogenic effects in endothelial cells through a phosphorylated myosin light chain-related mechanism. *PLOS ONE* **7**, e46510 (2012).
41. V. Pancholi, Multifunctional α-enolase: Its role in diseases. *Cell. Mol. Life Sci.* **58**, 902–920 (2001).
42. R. G. Fehon, A. I. McClatchey, A. Bretscher, Organizing the cell cortex: The role of ERM proteins. *Nat. Rev. Mol. Cell Biol.* **11**, 276–287 (2010).
43. K. L. Gould, A. Bretscher, F. S. Esch, T. Hunter, cDNA cloning and sequencing of the protein-tyrosine kinase substrate, ezrin, reveals homology to band 4.1. *EMBO J.* **8**, 4133–4142 (1989).
44. T. Mori, K. Kitano, S.-i. Terawaki, R. Maesaki, Y. Fukami, T. Hakoshima, Structural basis for CD44 recognition by ERM proteins. *J. Biol. Chem.* **283**, 29602–29612 (2008).
45. Y. Koga, M. Ikebe, A novel regulatory mechanism of myosin light chain phosphorylation via binding of 14-3-3 to myosin phosphatase. *Mol. Biol. Cell* **19**, 1062–1071 (2008).
46. J. E. Van Lierop, D. P. Wilson, J. P. Davis, S. Tikunova, C. Sutherland, M. P. Walsh, J. D. Johnson, Activation of smooth muscle myosin light chain kinase by calmodulin. Role of LYS^{30} and GLY^{40}. *J. Biol. Chem.* **277**, 6550–6558 (2002).
47. M. Wygrecka, L. M. Marsh, R. E. Morty, I. Henneke, A. Guenther, J. Lohmeyer, P. Markart, K. T. Preissner, Enolase-1 promotes plasminogen-mediated recruitment of monocytes to the acutely inflamed lung. *Blood* **113**, 5588–5598 (2009).
48. M. Braceland, M. F. McLoughlin, J. Tinsley, C. Wallace, D. Cockerill, M. McLaughlin, P. D. Eckersall, Serum enolase: A non-destructive biomarker of white skeletal myopathy during pancreas disease (PD) in Atlantic salmon *Salmo salar* L. *J. Fish Dis.* **38**, 821–831 (2015).
49. A. E. Michalska, K. H. A. Choo, Targeting and germ-line transmission of a null mutation at the metallothionein I and II loci in mouse. *Proc. Natl. Acad. Sci. U.S.A.* **90**, 8088–8092 (1993).
50. L.-M. Yin, G.-H. Jiang, Y. Wang, Y.-Y. Liu, W.-R. Jin, Z. Zhang, Y.-D. Xu, Y.-Q. Yang, Serial analysis of gene expression in a rat lung model of asthma. *Respirology* **13**, 972–982 (2008).
51. K. G. Tournoy, J. C. Kips, C. Schou, R. A. Pauwels, Airway eosinophilia is not a requirement for allergen-induced airway hyperresponsiveness. *Clin. Exp. Allergy* **30**, 79–85 (2000).
52. T. A. Doherty, P. Soroosh, N. Khorram, S. Fukuyama, P. Rosenthal, J. Y. Cho, P. S. Norris, H. Choi, S. Scheu, K. Pfeffer, B. L. Zuraw, C. F. Ware, D. H. Broide, M. Croft, The tumor necrosis factor family member LIGHT is a target for asthmatic airway remodeling. *Nat. Med.* **17**, 596–603 (2011).
53. M. J. Sanderson, Exploring lung physiology in health and disease with lung slices. *Pulm. Pharmacol. Ther.* **24**, 452–465 (2011).
54. L.-M. Yin, Y. Wei, Y. Wang, Y.-D. Xu, Y.-Q. Yang, Long term and standard incubations of WST-1 reagent reflect the same inhibitory trend of cell viability in rat airway smooth muscle cells. *Int. J. Med. Sci.* **10**, 68–72 (2013).
55. L.-M. Yin, X.-J. Han, T.-T. Duan, Y.-D. Xu, Y. Wang, L. Ulloa, Y.-Q. Yang, Decreased S100A9 expression promoted rat airway smooth muscle cell proliferation by stimulating ROS generation and inhibiting p38 MAPK. *Can. Respir. J.* **2016**, 1462563 (2016).
56. Y. Duan, J. Long, J. Chen, X. Jiang, J. Zhu, Y. Jin, F. Lin, J. Zhong, R. Xu, L. Mao, L. Deng, Overexpression of soluble ADAM33 promotes a hypercontractile phenotype of the airway smooth muscle cell in rat. *Exp. Cell Res.* **349**, 109–118 (2016).
57. M. Mikami, Y. Zhang, J. Danielsson, T. Joell, H. M. Yong, E. Townsend, S. Khurana, S. S. An, C. W. Emala, Impaired relaxation of airway smooth muscle in mice lacking the actin-binding protein gelsolin. *Am. J. Respir. Cell Mol. Biol.* **56**, 628–636 (2017).
58. J. P. Butler, I. M. Tolić-Nørrelykke, B. Fabry, J. J. Fredberg, Traction fields, moments, and strain energy that cells exert on their surroundings. *Am. J. Physiol. Cell Physiol.* **282**, C595–C605 (2002).
59. F. Lin, A. Song, J. Wu, X. Jiang, J. Long, J. Chen, Y. Duan, Y. Shi, L. Deng, ADAM33 protein expression and the mechanics of airway smooth muscle cells are highly correlated in ovalbumin-sensitized rats. *Mol. Med. Rep.* **8**, 1209–1215 (2013).
60. T. A. Halgren, R. B. Murphy, R. A. Friesner, H. S. Beard, L. L. Frye, W. T. Pollard, J. L. Banks, Glide: A new approach for rapid, accurate docking and scoring. 2. Enrichment factors in database screening. *J. Med. Chem.* **47**, 1750–1759 (2004).

Acknowledgments: We thank B.-F. Zhang and L.-F. Li for giving us breeding pairs of MT-KO mice; X. Shen and J. Chen for technical assistance in the Biacore analysis; J.-H. Zhu for preparing the ^{125}I-labeled protein; T. Zhang for advice on blood pressure measurement; L. Yang, X.-H. Zhao, and J. Zhang for the pharmacokinetic studies of TSG12; and J.-P. Zuo for advice on dosage determination. **Funding:** This study was supported by the National Natural Science Foundation of China (NSFC) (nos. 81574058, 81473760, and 81273435); Shanghai Talent Development Fund (201610); and Shanghai Key Research Program of Shanghai Municipal Commission of Health and Family Planning (ZY3-CCCX-3-3005). L.U. is supported by the NIH R01-GM114180, Eastern Scholar JZ2016010, and NSFC no. 81774429. **Author contributions:** L.-M.Y., Y.-D.X., L.-L.P., T.-T.D., J.-Y.L., W.-Q.W., N.G., X.-J.H., H.-Y.L., Y.P., and Y.W. conducted most of the experiments; Z.C., Z.X., and W.Z. contributed to molecular docking; G.-B.G. conducted the tissue distribution analysis; L.D. designed the experiments of OMTC and TFM; Y.-L.W. and S.H. participated in the data analysis; Y.-Q.Y., L.U., and L.-M.Y. wrote the manuscript and prepared the figures; and Y.-Q.Y. and L.U. designed the project and analyzed the data. **Competing interests:** The authors declare that they have no competing interests.

Submitted 6 February 2017
Resubmitted 11 September 2017
Accepted 1 November 2017
Published 7 February 2018
10.1126/scitranslmed.aam8604

Citation: L.-M. Yin, Y.-D. Xu, L.-L. Peng, T.-T. Duan, J.-Y. Liu, Z. Xu, W.-Q. Wang, N. Guan, X.-J. Han, H.-Y. Li, Y. Pang, Y. Wang, Z. Chen, W. Zhu, L. Deng, Y.-L. Wu, G.-B. Ge, S. Huang, L. Ulloa, Y.-Q. Yang, Transgelin-2 as a therapeutic target for asthmatic pulmonary resistance. *Sci. Transl. Med.* **10**, eaam8604 (2018).

Downloaded from http://stm.sciencemag.org/ by guest on July 7, 2021

Science Translational Medicine

Transgelin-2 as a therapeutic target for asthmatic pulmonary resistance

Lei-Miao Yin, Yu-Dong Xu, Ling-Ling Peng, Ting-Ting Duan, Jia-Yuan Liu, Zhijian Xu, Wen-Qian Wang, Nan Guan, Xiao-Jie Han, Hai-Yan Li, Yu Pang, Yu Wang, Zhaoqiang Chen, Weiliang Zhu, Linhong Deng, Ying-Li Wu, Guang-Bo Ge, Shuang Huang, Luis Ulloa and Yong-Qing Yang

Sci Transl Med **10**, eaam8604.
DOI: 10.1126/scitranslmed.aam8604

Tickling transgelin-2 for asthma relief

Asthmatics can be refractive to β_2-agonists, creating a need for new pathways to be targeted in this disease. Yin *et al*. discovered that the protein metallothionein-2 was able to reduce airway resistance in rodent asthma models. This improvement was mediated through transgelin-2, and they further studied a transgelin-2 agonist as a new asthma therapeutic. The agonist improved airway function in multiple preclinical asthma models and relaxed human airway smooth muscle cells. These data indicate that activating transgelin-2 for asthma treatment may be more effective than targeting β_2-adrenoceptors.

ARTICLE TOOLS http://stm.sciencemag.org/content/10/427/eaam8604

SUPPLEMENTARY MATERIALS http://stm.sciencemag.org/content/suppl/2018/02/05/10.427.eaam8604.DC1

RELATED CONTENT
http://stm.sciencemag.org/content/scitransmed/9/407/eaag2288.full
http://stm.sciencemag.org/content/scitransmed/8/362/362ra143.full
http://stm.sciencemag.org/content/scitransmed/8/359/359ra131.full
http://stm.sciencemag.org/content/scitransmed/10/455/eaaq0693.full
http://stm.sciencemag.org/content/scitransmed/10/457/eaar8477.full
http://stm.sciencemag.org/content/scitransmed/10/468/eaao2151.full
http://stm.sciencemag.org/content/scitransmed/11/479/eaao6451.full

REFERENCES This article cites 57 articles, 12 of which you can access for free
http://stm.sciencemag.org/content/10/427/eaam8604#BIBL

PERMISSIONS http://www.sciencemag.org/help/reprints-and-permissions

Use of this article is subject to the Terms of Service

Science Translational Medicine (ISSN 1946-6242) is published by the American Association for the Advancement of Science, 1200 New York Avenue NW, Washington, DC 20005. The title *Science Translational Medicine* is a registered trademark of AAAS.

Copyright © 2018 The Authors, some rights reserved; exclusive licensee American Association for the Advancement of Science. No claim to original U.S. Government Works

Downloaded from http://stm.sciencemag.org/ by guest on July 7, 2021